

## Coordinated Regulation of miR-155 and miR-146a Genes during Induction of Endotoxin Tolerance in Macrophages

This information is current as of November 19, 2015.

Christina Doxaki, Sotirios C. Kampranis, Aristides G. Eliopoulos, Charalampos Spilianakis and Christos Tsatsanis

*J Immunol* published online 4 November 2015  
<http://www.jimmunol.org/content/early/2015/11/04/jimmunol.1500615>

- 
- Supplementary Material** <http://www.jimmunol.org/content/suppl/2015/11/04/jimmunol.1500615.DCSupplemental.html>
- Subscriptions** Information about subscribing to *The Journal of Immunology* is online at: <http://jimmunol.org/subscriptions>
- Permissions** Submit copyright permission requests at: <http://www.aai.org/ji/copyright.html>
- Email Alerts** Receive free email-alerts when new articles cite this article. Sign up at: <http://jimmunol.org/cgi/alerts/etoc>



# Coordinated Regulation of miR-155 and miR-146a Genes during Induction of Endotoxin Tolerance in Macrophages

Christina Doxaki,\* Sotirios C. Kampranis,<sup>†</sup> Aristides G. Eliopoulos,<sup>‡,§</sup> Charalampos Spilianakis,<sup>§,¶</sup> and Christos Tsatsanis\*

Endotoxin tolerance occurs to protect the organism from hyperactivation of innate immune responses, primarily mediated by macrophages. Regulation of endotoxin tolerance occurs at multiple levels of cell responses and requires significant changes in gene expression. In the process of macrophage activation, induced expression of microRNA (miR)-155 and miR-146a contributes to the regulation of the inflammatory response and endotoxin tolerance. In this article, we demonstrate that expression of both miRNAs is coordinately regulated during endotoxin tolerance by a complex mechanism that involves monoallelic interchromosomal association, alterations in histone methyl marks, and transcription factor binding. Upon activation of naive macrophages, Histone3 was trimethylated at lysine4 and NFκBp65 was bound on both miR-155 and miR-146a gene loci. However, at the stage of endotoxin tolerance, both miR gene loci were occupied by C/EBPβ, NFκBp50, and the repressive Histone3 marks trimethylation of K9 of H3. DNA fluorescence in situ hybridization experiments revealed monoallelic interchromosomal colocalization of miR-155 and miR-146a gene loci at the stage of endotoxin tolerance, whereas RNA-DNA-fluorescence in situ hybridization experiments showed that the colocalized alleles were silenced, suggesting a common repression mechanism. Genetic ablation of Akt1, which is known to abrogate endotoxin tolerance, abolished induction of loci colocalization and C/EBPβ binding, further supporting that this mechanism occurs specifically in endotoxin tolerance. Overall, this study demonstrates that two miRNAs are coordinately regulated via gene colocalization at the three-dimensional chromatin space, same transcriptional machinery, and similar Histone3 methylation profile, contributing to the development of endotoxin tolerance. *The Journal of Immunology*, 2015, 195: 000–000.

Exposure of macrophages to endotoxin triggers a robust response resulting in the transcription of numerous genes that contribute to the inflammatory response. Expression of these genes is tightly regulated to avoid sustained activation, which can be detrimental to the host because it can result in endotoxin shock. Thus, macrophages enter the state of endotoxin tolerance, in which cells become hyporesponsive to TLR ligands and do not express most of the proinflammatory genes. At the stage of endotoxin tolerance, a different set of genes is expressed that includes anti-inflammatory cytokines and negative regulators of TLR signaling. Akt1 kinase is a negative regulator of TLR signals, which mediates its action via microRNAs (miRs) (1).

miRs are small, noncoding RNAs of ~19–22 nt that regulate multiple cellular functions via posttranslational control of mRNA expression, including ones involved in innate and adaptive immune responses. Several miRs (such as miR-146a, miR-221, miR-125b, miR-181c, miR-155 and let-7e, miR-98) have been identified to regulate TLR4 signaling and induce or maintain endotoxin tolerance (2–4). Among these, miR-155 and miR-146a have been implicated in both macrophage activation and development of endotoxin tolerance. Contribution of miR-146a and miR-155 in endotoxin tolerance has been demonstrated in vivo in mouse models and in human disease. miR-155 negatively contributed to the development of endotoxin tolerance (1), whereas miR-146a was indispensable for the development of endotoxin tolerance both in healthy conditions, such as tolerance to intestinal bacteria in neonates (5), and during septic shock (6). Contribution of these miRNAs in endotoxin shock and tolerance can also occur through their secretion in exosomes (7). In humans, miR-146a appears to be important in the development of innate immune tolerance observed in leukemic patients (8). Both miRs have attracted particular attention, because they are responsive to a plethora of inflammatory stimuli including TLR ligands, TNFα, IL-1b, type I and type II IFNs, or RANKL in different cell types, including macrophages (9–16). miR-155 and miR-146a target and repress several downstream TLR4 mediators such as TNF-α, PU.1, SHIP1, SOCS1 and TNFR-associated factor-6, IRAK1, and IRF5, respectively, highlighting their pivotal role in the development of endotoxin tolerance (1). Expression of both miRs has been associated with inflammatory diseases including rheumatoid arthritis (17, 18), systemic lupus erythematosus (19), nephropathy (20), atherosclerosis (21), infertility (22), periodontitis (23), and type 2 diabetes (24).

miRs are regulated at transcriptional and posttranscriptional levels (25). miR-155 is transcribed within the BIC gene, whereas

\*Laboratory of Clinical Chemistry, University of Crete Medical School, Heraklion 71003, Crete, Greece; <sup>†</sup>Laboratory of Biochemistry, University of Crete Medical School, Heraklion 71003, Crete, Greece; <sup>‡</sup>Molecular & Cellular Biology Laboratory, University of Crete Medical School, Heraklion 71003, Crete, Greece; <sup>§</sup>Institute of Molecular Biology and Biotechnology, Foundation for Research and Technology – Hellas, Heraklion 70013, Crete, Greece; and <sup>¶</sup>Department of Biology, University of Crete, Heraklion 71003, Crete, Greece

ORCID: 0000-0001-6208-1684 (S.C.K.); 0000-0003-0921-1923 (C.S.).

Received for publication March 13, 2015. Accepted for publication October 7, 2015.

This work was supported by Greek and European Union funds under APIS/TEIA Grant 2071, Association for International Cancer Research Grant AICR11-0505, and European Commission FP7 program Translational Potential Contract 285948.

Address correspondence and reprint requests to Prof. Christos Tsatsanis, Laboratory of Clinical Chemistry, School of Medicine, University of Crete, P.O. Box 2208, Heraklion 71003, Crete, Greece. E-mail address: tsatsani@med.uoc.gr

The online version of this article contains supplemental material.

Abbreviations used in this article: BAC, bacterial artificial chromosome; ChIP, chromatin immunoprecipitation; FISH, fluorescence in situ hybridization; H3K4me3, trimethylation of K4 of histone H3; H3K9me3, trimethylation of K9 of H3; miR, microRNA; pri-miR, primary microRNA; siRNA, small interfering RNA; TEPM, thioglycollate-elicited and LPS-stimulated peritoneal macrophage; WT, wild type.

Copyright © 2015 by The American Association of Immunologists, Inc. 0022-1767/15/\$25.00

miR-146a appears to be intergenic (10). Analysis of the gene promoters of these two miRNAs revealed that both are regulated by NF- $\kappa$ B (10, 26, 27), suggesting a common transcriptional regulatory mechanism.

A complex biological process such as endotoxin tolerance requires significant changes in gene expression via specific transcription factors and histone modifications to ensure temporal gene regulation (28, 29). Gene-specific regulation occurs at the chromatin level and includes nucleosome remodeling and covalent histone modifications. Histone methylation, as a mechanism for modifying chromatin structure, is associated with gene regulation. Trimethylation of lysine H3K4 marks transcriptionally active genes, whereas trimethylation of lysine H3K9 is associated with transcriptional repression and is generally found in closed inactive chromatin (30–32). Upon endotoxin tolerance, several genes appear to be regulated at the chromatin level, indicating the presence of an epigenetic mechanism (33–36). However, no information is yet available on histone modification changes of miRNA genes in the process of endotoxin tolerance.

Recent evidence has shown that genes contributing to a particular cellular function or cell fate can be coordinately regulated through long-range chromatin interactions (37–44). According to this mechanism, genes present on the same or different chromosomes come in close proximity and use the same transcription factory by looping out of their chromosome territories. Thus, genes are dynamically organized into shared nuclear subcompartments, which ensure a common regulation of their transcription. An example of such association is that of the Th2 gene locus with the loci harboring the Th2 cytokines IL-4, IL-5, and IL-13, which are located on different chromosomes (44). These associated gene loci use common transcription factors to secure timely and coordinate gene regulation, necessary for massive changes in gene expression that occur under conditions such as macrophage activation and endotoxin tolerance. However, it is not known whether chromatin interactions between gene loci harboring microRNAs take place. In addition, whether interchromosomal associations facilitate expression or silencing of genes during the development of endotoxin tolerance in macrophages remains unknown.

In this study, we analyzed the mechanism that controls expression of miR-155 and miR-146a in response to LPS in naive and endotoxin-tolerant macrophages using the RAW264.7 cell line and mouse primary macrophages. We found that both mature and immature primary microRNA (pri-miR) miR-155 and miR-146a were induced upon LPS stimulation of naive macrophages, whereas in endotoxin-tolerant macrophages their expression was induced at much lower levels. Chromatin immunoprecipitation (ChIP) analysis revealed that their genomic loci are regulated by the same transcription factors, namely, NF- $\kappa$ B and C/EBP $\beta$ . Fluorescence in situ hybridization (FISH) experiments showed a monoallelic interchromosomal association between miR-155 and miR-146a gene loci at the stage of endotoxin tolerance, which conferred gene silencing. Genetic ablation of Akt1, which was used as a genetic tool to abrogate endotoxin tolerance, changed miR-155 and miR-146a expression, altered NF- $\kappa$ B/p65 and C/EBP $\beta$  binding on their promoters, and inhibited the induction of colocalization of miR-155 and miR-146a gene loci, further highlighting the significance of this association.

## Materials and Methods

### Animals

C57BL/6 mice were purchased from the Hellenic Pasteur Institute (Athens, Greece). Akt1<sup>-/-</sup> and Akt1<sup>+/+</sup> mice (45, 46) were housed at the University of Crete School of Medicine, Greece. All procedures described later were approved by the Animal Care Committee of the University of Crete School

of Medicine (Heraklion, Crete, Greece) and from the Veterinary Department of the Region of Crete (Heraklion, Crete, Greece).

### Cell culture

The murine macrophage cell line RAW264.7 and primary murine thioglycollate-elicited peritoneal macrophages were cultured as previously described (47) in macrophage complete medium (DMEM; Life Technologies, Carlsbad, CA) supplemented with 10% (v/v) FBS, 10 mM L-glutamine, 100 IU/ml penicillin, and 100  $\mu$ g/ml streptomycin. RAW264.7 cells were tested by FISH analysis and found to be diploid at least on chromosomes 7, 8, 11, 16, and 17, and were kindly provided by Prof. P. Tsichlis (Tufts Medical School, Boston, MA). *E. coli*-derived LPS (100 ng/ml; O111:B4; catalog no. L2630; Sigma-Aldrich) was used as described in the Results. Cells were harvested and supernatants were collected at the indicated time points of LPS incubation and stored at  $-80^{\circ}\text{C}$  until assayed for cytokine levels. Cell pellets were washed in PBS and stored at  $-80^{\circ}\text{C}$  for total RNA extraction and subsequent analysis.

### ELISA

Cytokine concentration in serum for TNF- $\alpha$  and IL-10 was determined by ELISA at the indicated time points using ELISA kits (R&D Systems), according to the manufacturer's instructions.

### Transfection

Transient transfection using the Lipofectamine reagent (RNAimax; Life Technologies) was performed as per the manufacturer's instructions and as described previously (13, 48, 49). In short, a unique RNAi molecule was used in each well before transfection and combined with diluted lipofectamine to form complexes. Cells were added directly to the complexes, and transfection was performed while cells were attaching on to the well. A total of  $1 \times 10^5$  macrophages/well was transfected with either 30 nM small interfering RNA (siRNA) for C/EBP $\beta$  (designed in Cenix Bioscience, Dresden, Germany) or negative control dsRNA in 24-well tissue-culture plates in a volume of 500  $\mu$ l serum-free/antibiotic-free DMEM culture media. Cells were incubated at  $37^{\circ}\text{C}$  for 24 h and then the medium was replaced with the one before transfection. Transfection efficiency and biological effect were assessed 48 h posttransfection.

### In vitro induction of endotoxin tolerance

An LPS-tolerance cell model using either the murine macrophage cell line RAW 264.7 or primary thioglycollate-elicited peritoneal macrophages was adapted from methods previously described with minor modifications (13). In brief, cells were cultured in complete culture medium [DMEM (Life Technologies) supplemented with 10% (v/v) FBS, 10 mM L-glutamine, 100 IU/ml penicillin, and 100  $\mu$ g/ml streptomycin] for 1 d, and viability was monitored by trypan blue staining and was found to be  $\sim 99\%$ . Cells ( $300 \times 10^3$  cells/ml) were seeded in 12- or 24-well tissue-culture plates in a volume of 1 ml fresh complete medium and incubated with LPS (100 ng/ml) for 18 h. After two washes with tissue culture grade  $1 \times \text{PBS}$ , cells were cultured in complete culture media in a  $\text{CO}_2$  incubator for 2 h at  $37^{\circ}\text{C}$ . In case of restimulation, LPS (100 ng/ml, final concentration) was added for 2 h. Supernatants and cell pellets were harvested and stored at  $-80^{\circ}\text{C}$  until assayed.

### RNA and miRNA isolation and quantitative PCR

RNA from RAW264.7 macrophages or from primary thioglycollate-elicited peritoneal macrophages was isolated using the TRIzol reagent (Life Technologies). One microgram of total RNA after DNase treatment was used for cDNA synthesis (TAKARA, Shiga, Japan). The following oligonucleotides were used in semiquantitative RT-PCR approach: Pri-miR-155; Fwd: 5'-ACCCTGCTGGATGAACGTAG-3'; Rev: 5'-CATGTGGGCTTGAAGTTGAG-3'; Pri-miR-146a; Fwd: 5'-CACGGACCTGAAGAACTGG-3'; Rev: 5'-AGAAATGAAATTAGAACACATCAATCC-3'; C/EBP $\beta$ ; Fwd: 5'-GGGGTTGTTGATGTTTTTGGTT-3'; Rev: 5'-TCACCTTAATGCTCGAAACGGA-3'; Ribosomal Protein S9; Fwd: 5'-GCTAGACGAGGAAGGATCCCC-3'; Rev: 5'-CAGGCCAGCTTAAAGACCT-3'; Hprt1; Fwd: 5'-CTGGTGAAGGACCTCTCG-3'; Rev: 5'-TGAAGTACTCATATAGTCAAGGGCA-3'. Ribosomal Protein S9 and Hprt1 served as control housekeeping genes. Annealing was carried out at  $60^{\circ}\text{C}$  for 30 s, extension at  $72^{\circ}\text{C}$  for 30 s, and denaturation at  $95^{\circ}\text{C}$  for 15 s for 40 cycles in a 7500 Fast Real-Time PCR System (Life Technologies/Applied Biosystems). The amplification efficiencies were the same as the one of RSP9 or Hprt1 as indicated by the standard curves of amplification, allowing us to use the following formula: fold difference =  $2^{-(\Delta\text{CtA} - \Delta\text{CtB})}$ , where Ct is the cycle threshold. Reactions were performed in triplicate for statistical evaluation. To isolate miRNAs from RAW264.7 or thioglycollate-elicited peritoneal macrophages, we isolated total RNA as described earlier. For



cDNA synthesis and quantitative PCR of specific miRNAs, the following TaqMan MicroRNA Assays (Life Technologies) were used: mmu-miR-155; UAAUAGCUAAUUGUGAUAGGGGU; hsa-miR-146a; UGAGAACUG-AAUUCUAGGGGU; SnoRNA135; CUAAAUAUGCUGGAUUUACCGG-CAGAUUGGUAGUGGUG. SnoRNA135 served as housekeeping miRNA. Annealing and extension was carried out at 60°C for 30 s and denaturation at 95°C for 15 s for 40 cycles in a 7500 Fast Real-Time PCR System (Life Technologies).

### DNA and DNA-RNA FISH

Cells attached onto poly-L-lysine-coated glass coverslips were incubated for 3 min in cytoskeletal buffer (100 mM NaCl, 300 mM sucrose, 3 mM MgCl<sub>2</sub>, 10 mM PIPES, 0.5% Triton X-100), fixed with 4% paraformaldehyde/1×PBS for 10 min, washed three times with 1×PBS, and stored in 70% ethanol at −20°C overnight. Hybridization was carried out in 50% formamide, 2×SSC, 10% dextran sulfate, 1 μg mouse Cot-1 (Invitrogen), and 100 ng fluorescently labeled bacterial artificial chromosome (BAC) probe, and after a 5-min denaturation of genomic DNA at 73°C, coverslips were incubated for 16 h at 37°C. Slides were washed three times for 5 min each in 2×SSC and mounted in Prolong Gold antifade reagent supplemented with DAPI (Invitrogen). For the generation of fluorescently labeled DNA probes, 2 μg BAC DNA [(miR-146a ID for BAC clone: RP23-390G17); (miR-155 ID for BAC clone: RP24-278G19); (let-7e ID for BAC clone: RP24-308G19); and (TNF-α ID for BAC clone: RP23-446C22)] were labeled using a Nick translation kit (11745808910; Roche) supplemented with either 0.025 mM Spectrum Orange dUTP (Vysis), 0.025 mM Spectrum Green dUTP (Vysis), or 0.025 mM OBEA dCTP-647 (Invitrogen). The following primers were used in PCRs to confirm the presence of each gene of interest in the BAC clones: MiR-146a: Fwd 5'-GGCCTTCAGAGTTTGTTCAC-3', Rev 5'-GGCCTCATCTGGA-GAGTCTG-3'; MiR-155: Fwd 5'-TTGCTGAAGGCTGTATGCTG-3', Rev 5'-ATCCAGCAGGGTGACTCTTG-3'; Let-7e: Fwd 5'-AAAGAAACAAGA-AGACGGAC-3', Rev 5'-ATCCCTTAGAGAAGACAATCTG-3'; and TNF-α: Fwd 5'-TTCTCTCTTATCTCTCATGC-3', Rev 5'-TGACTAAACATCC-TTCGTCG-3'. To detect DNA and RNA by FISH, we incubated cells attached onto poly-L-lysine-coated coverslips for 3 min in cytoskeletal buffer (100 mM NaCl, 300 mM sucrose, 3 mM MgCl<sub>2</sub>, 10 mM PIPES, 0.5% Triton X-100, 1 mM EGTA, and 2 mM vanadyl-ribonucleoside complex), fixed with 4% paraformaldehyde/1×PBS for 10 min, washed three times with 70% ethanol, and stored in 70% ethanol at −20°C overnight. Hybridization was performed with biotinylated probes for 16 h at 37°C after a 5-min denaturation at 73°C. The coverslips were washed at 37°C sequentially with 2×SSC/50% formamide, 2×SSC, 1×SSC, and 4×SSC. RNA signals were amplified using the Renaissance TSA Biotin System (PerkinElmer). The biotinylated DNA probes were prepared as follows: 1000-bp genomic region containing the pri-miR-155 or pri-miR-146a RNA sequence was PCR-amplified and cloned in a PCRII-TOPO TA cloning vector (Life Technologies). Nick-translated biotin-labeled cloned DNA was used as a probe for the detection of the miR RNA signals. The following pairs of primers were used for the amplification of the miR loci: Pri-miR-155: 5'-ACCCTGCTGGATGAACGCTAG-3'; 5'-CATGTGGGCTT-GAAGTTGAG-3'; Pri-miR-146a: 5'-AGCACTGTCAACCTGACACA-3'; 5'-GGACCAGCAGTCTCTTGTAT-3'.

### Microscopy and image analysis

FISH signals were examined on a Leica SP8 confocal microscope unit, and image stacks were captured on a CCD camera with a step of 250 nm. The distances of DNA FISH signals were further analyzed using the Velocity image analysis software (Improvision) by two independent investigators. Photomicrographs represent merged confocal images, but statistical analysis for locus proximity has been performed for images of cells with preserved three-dimensional structure. As colocalized we considered DNA FISH signals that were either touching (adjacent pixels) or overlapping (overlapping pixels).

### ChIP

Chromatin from 15 × 10<sup>6</sup> RAW264.7 cells or primary peritoneal thioglycollate-elicited macrophages was prepared by fixation of the cell culture with 1/10 vol formaldehyde-containing buffer (11% formaldehyde, 100 mM NaCl, 1 mM EDTA, 0.5 mM EGTA, 50 mM Hepes pH 8.0) and incubation for 10 min at room temperature. For quenching the cross-linking, glycine was added for 5 min at room temperature to a final concentration of 125 mM directly in the culture media. Scraping and transfer of cells to a 15-ml conical tube and two washes with ice cold 1×PBS (supplemented with 1 mM PMSF) followed, and the cell pellet was incubated with 10 ml cell lysis buffer [5 mM PIPES (pH 8.0), 85 mM KCl, 0.5% Nonidet P-40, 1 mM PMSF, complete protease inhibitors] for 10 min

on ice. The cells were lysed with 800 μl SDS lysis buffer (1% SDS, 10 mM EDTA, 50 mM Tris-HCl pH 8.1) for 10 min on ice. Chromatin was sonicated to an average length of DNA 500–1000 bp. Immunoprecipitation was performed with the equivalent of 3–4 × 10<sup>6</sup> cells/sample, diluted 10 times with ChIP dilution buffer (0.01% SDS, 1.1% Triton X-100, 1.2 mM EDTA, 16.7 mM Tris-HCl pH 8.0, 167 mM NaCl supplemented with protease inhibitors) and 5 μg of each Ab. Samples were rotated at 4°C overnight (1% of chromatin input was kept). The next day each sample was mixed with 20 μl magnetic beads and was rotated for 2 h at 4°C. Immunoprecipitated material was incubated for 5 min with each of the following buffers: low-salt Wash Buffer A (0.1% SDS, 1% Triton X-100, 2 mM EDTA, 20 mM Tris-HCl pH 8.0, 150 mM NaCl supplemented with protease inhibitors), high-salt Wash Buffer B (0.1% SDS, 1% Triton X-100, 2 mM EDTA, 20 mM Tris-HCl pH 8.8, 500 mM NaCl supplemented with protease inhibitors), Buffer C [20 mM Tris-HCl (pH 8.0), 250 mM LiCl, 1 mM EDTA, 0.5% Nonidet P-40, 0.5% Na-Deoxycholate, 0.5 PMSF supplemented with Protease inhibitors], and once with Tris-EDTA buffer, pH 8.0. After the last wash, samples were incubated with proteinase K (200 mg/ml), 0.5% SDS in Tris-EDTA buffer for 2 h at 55°C, and then were incubated overnight at 65°C for the reversal of formaldehyde cross-links. DNA was purified with phenol/chloroform extraction and was precipitated with ethanol (1% glycogen and 10% CH<sub>3</sub>COONa). Immunoprecipitated DNA was resuspended in 40 μl of 100 mM Tris-HCl pH 7.5. Five percent of the immunoprecipitated DNA was used in quantitative PCR analysis, and data have been normalized using the formula: 100 × 2<sup>(Ct adjusted input − Ct IP)</sup>. The Abs that were used in the ChIP experiments were the following: RNA Polymerase II N-20 (sc899; Santa Cruz Biotechnology); NF-κB p65 Ab-c-20x (sc 372x; Santa Cruz Biotechnology); NF-κB p50 Ab-c-19 (sc 1190; Santa Cruz Biotechnology); C/EBPβ Ab-c-19 (sc 150x; Santa Cruz Biotechnology); Anti-Histone H3 Ab (D2B12)/#4620 Cell Signaling (chip-formulated); Anti-Histone H3 (trimethyl K4) Ab (ab8580; Abcam); Anti-Histone (trimethyl K9) Ab (ab6001; Abcam); Anti-Histone (trimethyl K27) Ab (catalog no. 07-449; Upstate). The following primer pairs were used for the amplification of the miR-155 and miR-146a promoter regions in the ChIP experiments: MiR-146a: Fwd 5'-ACTCCGT-CTTGCAACGAAC-3', Rev 5'-TCCCTTCTCAATCCCTCCT-3'; MiR-155: Fwd 5'-TTTCGAGCCGAGGTTCAC-3', Rev 5'-CGGCGACCCCTTTATAGCCC-3'.

### Statistical analysis

All values were expressed as mean ± SD. Comparison of results between different groups was performed by nonparametric analysis (Mann-Whitney and *t* test where applicable), using GraphPadInStat (GraphPad Software, San Diego, CA). A *p* value <0.05 was considered significant.

## Results

### Induction of miR-155 and miR-146a expression by LPS is reduced at the stage of endotoxin tolerance

LPS stimulation activates macrophages and induces expression of both miR-155 and miR-146a. Time-course analysis of miR-155 and miR-146a expression upon LPS treatment of RAW264.7 macrophages revealed that pri-miR-155 and pri-miR-146a reached a peak between 2 and 4 h and then their levels declined (Fig. 1A). The mature forms of the same miRNAs were induced simultaneously; miR-155 peaked at 18 h and declined thereafter, reaching the levels of miR-146a, suggesting that there is an additional, post-transcriptional level of regulation (Fig. 1B). When macrophages became endotoxin tolerant, following an established protocol according to which they become hyporesponsive to a subsequent LPS stimulation (Supplemental Fig. 1) (13), mature miR-155 and miR-146a levels were not further increased (Fig. 1B), whereas their transcripts were only moderately induced (Fig. 1C). These findings suggested the potential coordinated transcriptional regulation of miR-155 and miR-146a gene expression at the stage of endotoxin tolerance.

### Transcriptional regulation and H3 methylation status of miR-155 and miR-146a genes in naive and endotoxin-tolerant macrophages

To evaluate the status of the transcriptional machinery of miR-155 and miR-146a genes at the endotoxin-tolerant state of macro-

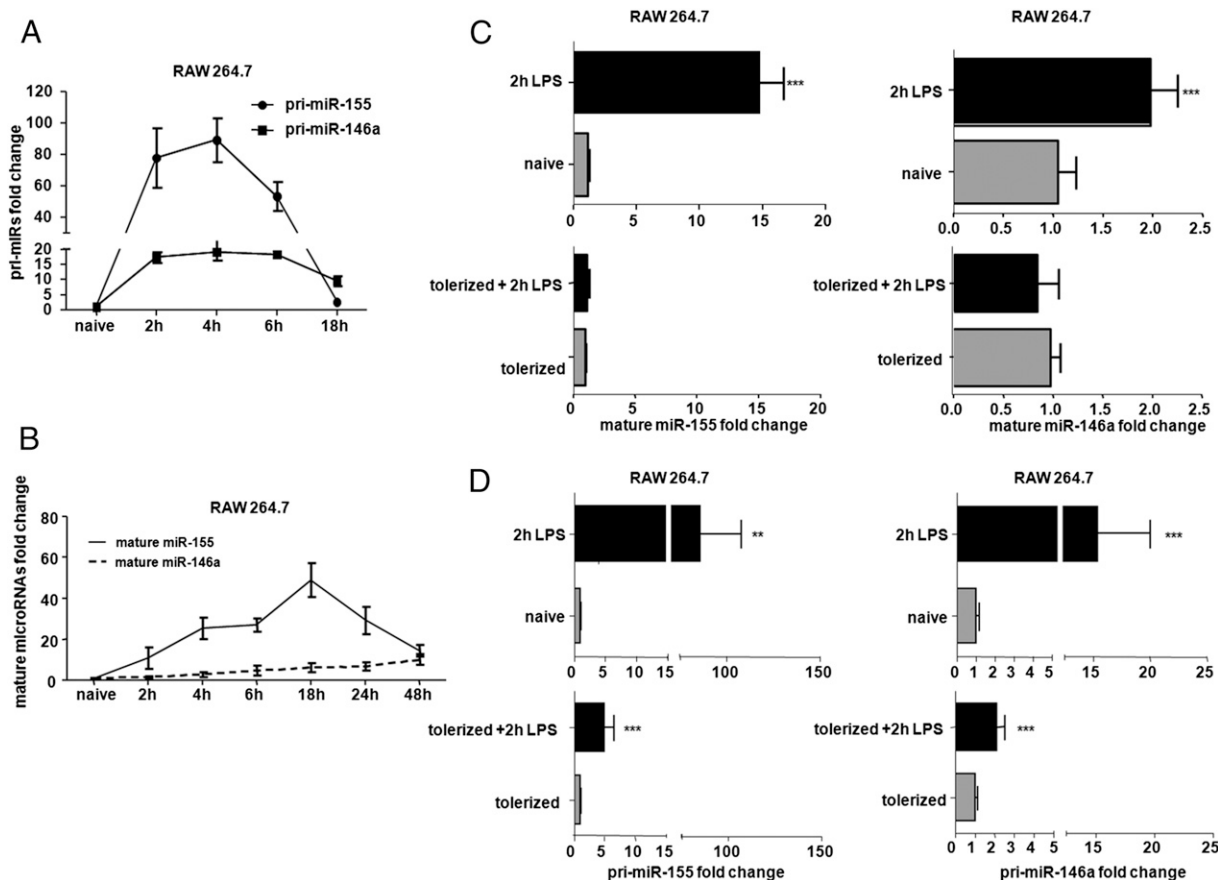


**FIGURE 1.** miR-155 and miR-146a are not further induced by LPS at the stage of endotoxin tolerance. **(A)** The microRNAs transcripts for pri-miR-155 and pri-miR-146a were measured in stimulated RAW264.7 macrophages with LPS for the indicated time course. **(B)** The mature forms of miR-155 and miR-146a were measured in stimulated RAW264.7 macrophages with LPS for the indicated time course. **(C)** Steady-state RNA levels of mature miR-155 and miR-146a were measured in naive, in 2-h-LPS-activated, in endotoxin-tolerant, and in endotoxin-tolerant RAW264.7 macrophages restimulated for 2 h with LPS. **(D)** Pri-miR-155 and pri-miR-146a levels were measured in 2-h-LPS-activated, in endotoxin-tolerant, and in endotoxin-tolerant RAW264.7 macrophages restimulated for 2 h with LPS. Results represent three independent experiments ( $\pm$  SD). \*\* $p = 0.01$ , \*\*\* $p = 0.001$  compared with unstimulated or tolerant macrophages.

phages, we assessed the binding of RNA Polymerase II to their respective regulatory sequences using ChIP assays. RNA Polymerase II binding was augmented after 2-h LPS activation of naive macrophages and was reduced in tolerant or LPS-restimulated tolerant macrophages (Fig. 2A), in accordance with the reduced transcription of these miRs. Accordingly, trimethylation of K4 of histone H3 (H3K4me3), a mark associated with transcriptionally active chromatin was increased upon LPS stimulation of naive macrophages on both miR-155 and miR-146a promoters (Fig. 2B). H3K4me3 levels dropped upon LPS restimulation of tolerant macrophages, supporting a negative regulation of miR expression at that stage. In agreement with this observation, trimethylation of K9 of H3 (H3K9me3), found in silenced chromatin, was increased in the tolerant state and then dropped upon LPS restimulation (Fig. 2C). These findings show that both miRs obtain the activation mark H3K4me3 at the initial activation stage, whereas at the stage of endotoxin tolerance, both miR promoters were occupied by the repressive mark H3K9me3. Upon LPS restimulation of endotoxin-tolerant macrophages, the ratio H3K4me3 to H3K9me3 did not change, whereas both active and repressive histone methylation marks were reduced.

To identify transcription factors likely involved in the regulation of both miR-155 and miR-146a transcription, we analyzed their promoter regions, based on published data (10, 50, 51) and on relevant software (Genomatix, Rvista, Patch) (Fig. 3A). Both regulatory sequences included putative NF- $\kappa$ B and C/EBP $\beta$  binding

sites. ChIP experiments revealed that binding of p65, the activation component of the NF- $\kappa$ B complex, increased upon LPS-stimulated macrophages and not in LPS-tolerant macrophages. However, p50, the inhibitory component of the NF- $\kappa$ B complex, was bound on both promoters at the stage of endotoxin tolerance, but not upon LPS treatment of naive macrophages (Fig. 3B, 3C). C/EBP $\beta$ , a transcription factor associated with both transcriptional activation and suppression, including silencing of miR-155 (52, 53), was bound on the promoter of both miRNA genes in the naive state. C/EBP $\beta$  binding was reduced upon LPS activation only on the miR-155 promoter, and it occupied both miR-155 and miR-146a promoters in tolerant and restimulated tolerant macrophages (Fig. 3D). Knockdown of C/EBP $\beta$  in RAW264.7 cells (Supplemental Fig. 2A) resulted in upregulation of pri-miR-155 and pri-miR-146a in endotoxin-tolerant macrophages, indicating that C/EBP $\beta$  participates in transcriptional suppression complexes at the stage of LPS tolerance (Fig. 3E). Furthermore, C/EBP $\beta$  depletion resulted in increased TNF- $\alpha$  secretion upon LPS stimulation, supporting the role of C/EBP $\beta$  as a negative transcriptional regulator (Supplemental Fig. 2B).

#### *Monoallelic colocalization of miR-155 and miR-146a gene loci in endotoxin-tolerant macrophages*

Gene transcription can be coordinately regulated via the same transcription complex when two gene loci are found in close proximity (43). Because both miRNAs were regulated by the same transcription factors and responded similarly to LPS at the stage of

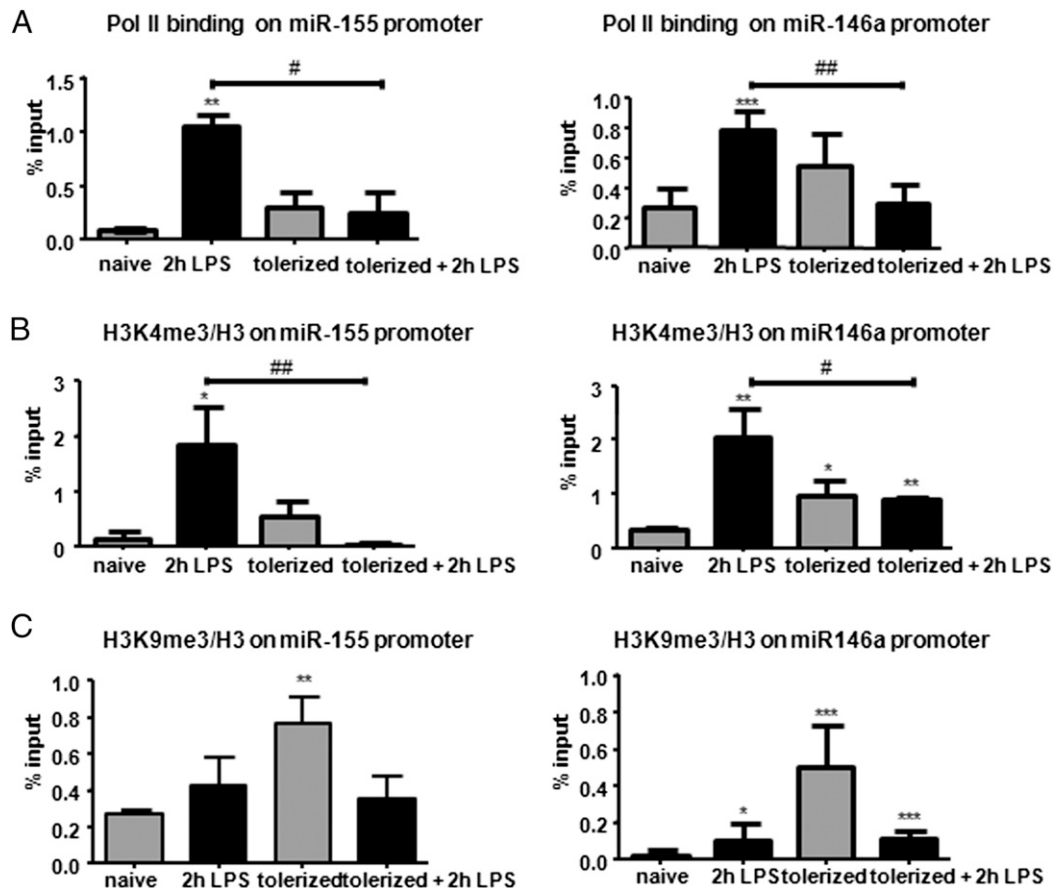


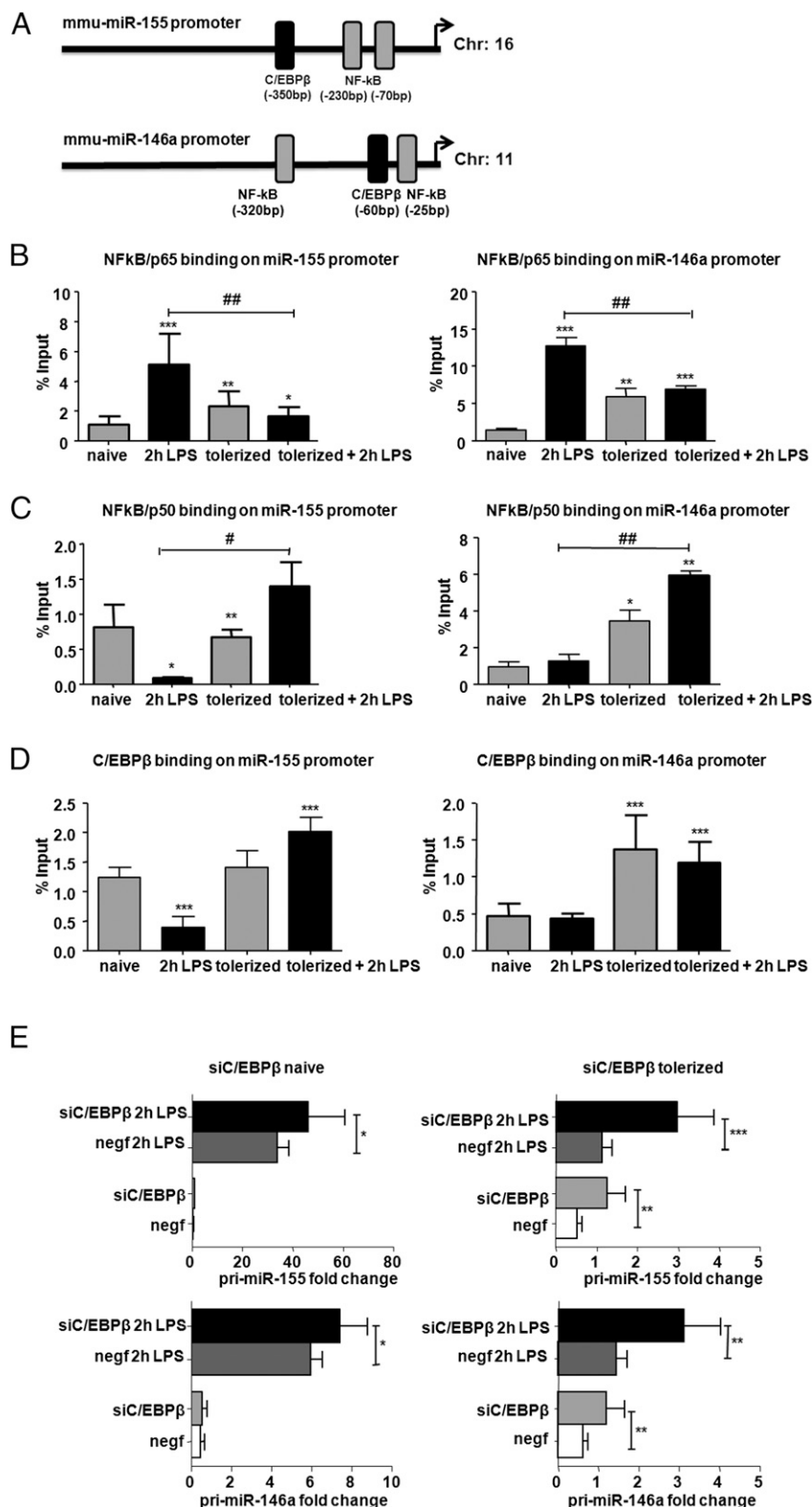
**FIGURE 2.** H3 methylation status of miR-155 and miR-146a genes in naive and endotoxin-tolerant macrophages. Cell lysates from RAW264.7 macrophages at the naive state, following 2-h LPS activation, at endotoxin-tolerant state, and following 2-h LPS activation of endotoxin-tolerant cells were used in ChIP experiments with an mAb directed to (A) RNA Polymerase II, (B) H3K4me3, and (C) H3K9me3. Precipitated DNA was amplified using primer pairs against a region of the miR-155 and miR-146a promoters. All H3K modifications were normalized against total levels of H3. Results represent three independent experiments ( $\pm$  SD). \* $p$  = 0.05, \*\* $p$  = 0.01, \*\*\* $p$  = 0.001 compared with unstimulated macrophages; # $p$  = 0.05, ## $p$  = 0.01 compared with cells activated with LPS for 2 h.

endotoxin tolerance, we examined whether miR-155 and miR-146a gene loci come in close proximity. For this purpose, we analyzed the subnuclear localization pattern of the gene loci for miR-155/bic and miR-146a, which are located on mouse chromosomes 16 and 11 respectively, by DNA FISH. Assessment of the percentage of cells bearing colocalized FISH signals of the two miR loci based on the distance between the two FISH signals. The results showed that the aforementioned loci came into proximity upon endotoxin tolerance in RAW264.7 macrophages, and this colocalization became even more prominent in LPS-restimulated tolerant macrophages (Fig. 4A), suggesting interchromosomal association. The observed differences in the percentage of cells harboring colocalized miR-155 and miR-146a alleles were not due to differences in the cell volume, because this was not found to decrease at the LPS-tolerant stage (Supplemental Fig. 3A). The observed colocalization of the two loci was monoallelic in the conditions analyzed (Fig. 4A), indicating that only one of the two alleles of each miRNA locus participates in this association. Analyzing the subnuclear localization pattern of gene loci for let-7e, an miRNA known to participate in macrophage activation and endotoxin tolerance, no colocalization with miR-155 gene locus was observed, indicating that the association of miR-155 and miR-146a is specific rather than coincidental (Supplemental Fig. 3B). In addition, FISH analysis of miR-155, miR-146a, and TNF- $\alpha$ , a cytokine gene known to be silenced at the stage of endotoxin tolerance, did not reveal colocalization of

the TNF- $\alpha$  locus with any of the miRNA genes (data not shown), suggesting that associations may be restricted to certain groups of genes.

Although biallelic gene expression can be considered the default state, several cases have been reported where genes are transcribed only from one of the two alleles, whereas the other remains in a heterochromatic inactive state (54–57). To determine the allelic expression profile of miR-155 and miR-146a, we performed RNA-DNA FISH experiments in naive, 2-h LPS-stimulated, endotoxin-tolerant and LPS-restimulated, endotoxin-tolerant RAW264.7 macrophages, detecting either the miR-155 transcript (RNA) and the primary miR-155 gene locus (DNA) or the primary miR-146a transcript (RNA) and the miR-146a gene locus (DNA) (Supplemental Fig. 3C). We measured the percentage of cells expressing miR-155 or miR-146a from one or both alleles. We found that the monoallelic-to-biallelic expression ratio of miR-155 and miR-146a was increased upon induction of endotoxin tolerance. The percentage of cells with biallelic expression of miR-155 and miR-146a was significantly reduced from 25 to 2% and 20 to 4.5%, respectively (Supplemental Fig. 3D, 3E). To examine whether the interchromosomal association of the two miR loci occurred in transcribed or silenced alleles, we performed RNA-DNA FISH experiments simultaneously detecting the miR-155 or miR-146a primary transcript together with the miR-155 and miR-146a gene loci (Fig. 4B, 4C). The results showed that colocalization occurred primarily between alleles that were not transcribed, which was

**FIGURE 3.** Transcriptional regulation of miR-155 and miR-146a genes in naive and endotoxin-tolerant macrophages. **(A)** miR-155 and miR-146a promoters include similar transcription factor binding sites. Schematic representations of miR-155 (*upper*) and miR-146a (*lower*) gene loci on mouse chromosomes 16 and 11 are shown, respectively. Putative binding sites for NF- $\kappa$ B (gray) and C/EBP $\beta$  (black) transcription factors are shown (boxes). **(B–D)** Cell lysates from RAW264.7 macrophages at the naive state, following 2-h LPS activation, at endotoxin-tolerant state, and following 2-h LPS activation of endotoxin-tolerant cells were used in ChIP experiments with an mAb directed to (B) NF- $\kappa$ B/p65, (C) NF- $\kappa$ B/p50, and (D) C/EBP $\beta$ . Precipitated DNA was amplified using primer pairs against a region of the miR-155 and miR-146a promoters. Results represent three independent experiments ( $\pm$  SD). \* $p$  = 0.05, \*\* $p$  = 0.01, \*\*\* $p$  = 0.001 compared with unstimulated macrophages; # $p$  = 0.05, ## $p$  = 0.01 compared with cells activated with LPS for 2 h. **(E)** Pri-miR-155 and pri-miR-146a RNA levels were measured in naive, in 2-h-LPS-activated, in endotoxin-tolerant, and in endotoxin-tolerant RAW264.7 macrophages restimulated for 2 h with LPS, following transfection with siRNAs for C/EBP $\beta$  or control siRNA (siNegF). Results represent three independent experiments ( $\pm$  SD). \* $p$  = 0.05, \*\* $p$  = 0.01, \*\*\* $p$  = 0.001 compared with transfected macrophages with siNegF.



more prominent when endotoxin-tolerant cells were restimulated with LPS (Fig. 4B, 4C). This observation indicated that the close proximity of miR-155 and miR-146a gene loci resulted in silencing of miRNA transcription.

The reduction of miRNA expression in endotoxin-tolerant cells was greater than what can be accounted from silencing one allele, suggesting that transcription from the nonlocalized allele may also be suppressed and remain in a state of low expression. At the

stage of endotoxin tolerance, binding of the transcriptional repressors C/EBP $\beta$  and NF- $\kappa$ B p50 was increased, whereas binding of the transcriptional activator NF- $\kappa$ B p65 was decreased. Accordingly, in endotoxin-tolerant cells, the ratio of p65/p50 bound on miR-155 locus decreased 11-fold and the same ratio decreased 6-fold on miR-146a locus (Supplemental Fig. 4A). Therefore, the NF- $\kappa$ B complexes in endotoxin-tolerant cells favored the inhibitory p50 isoform, suggesting that the alleles that are not colo-



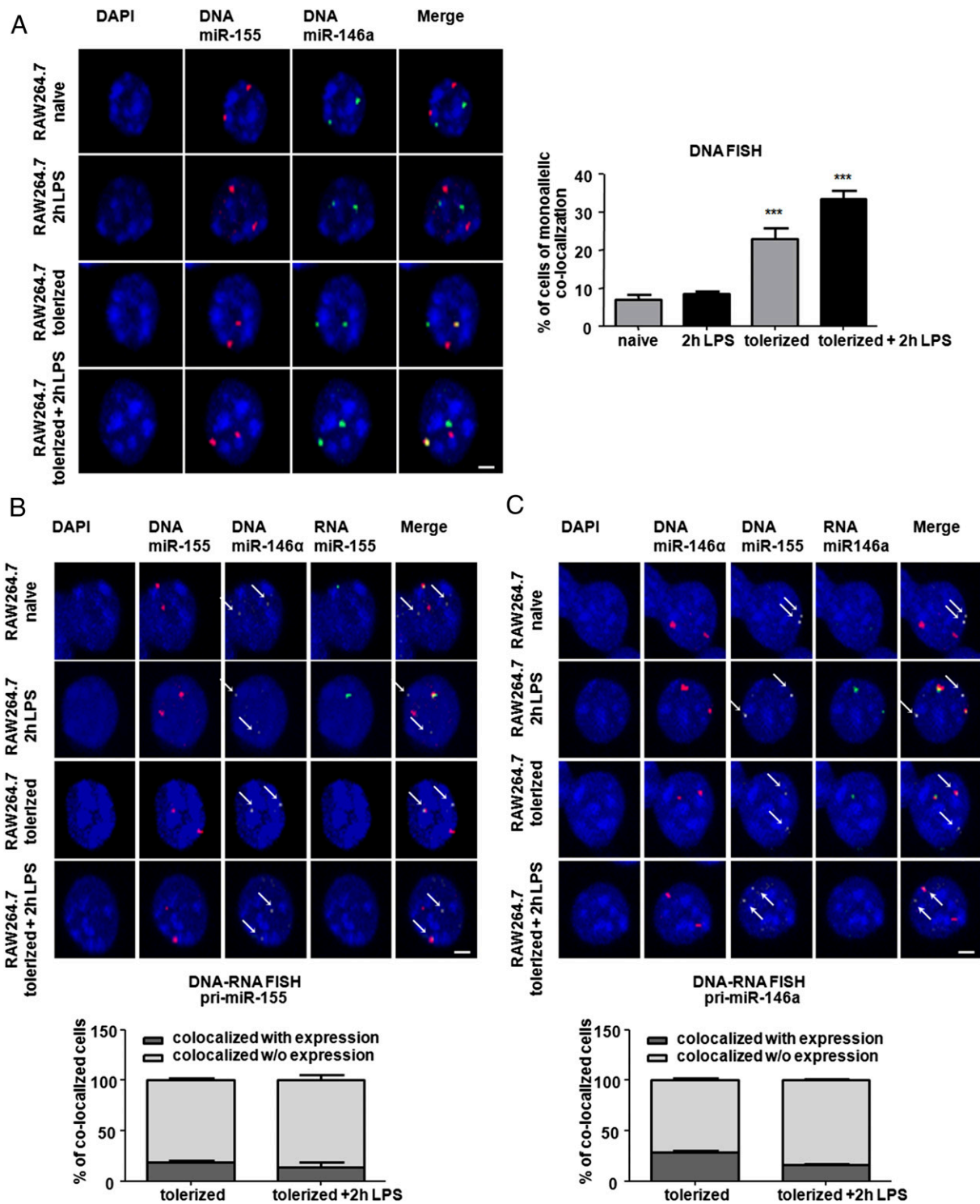


**FIGURE 4.** Monoallelic colocalization of miR-155 and miR-146a gene loci. **(A)** DNA FISH experiments were performed in naive, in 2-h-LPS-activated, in endotoxin-tolerant, and in endotoxin-tolerant RAW264.7 macrophages restimulated for 2 h with LPS, for the detection of miR-155 and miR-146a gene loci. Graphs depict the percentage of cells harboring miR-155 and miR-146a gene loci colocalization. The measurements were performed in three-dimensionally preserved cell nuclei, and 1000 cells were scored totally in three independent experiments for each state ( $\pm$  SD). \*\*\* $p$  = 0.001 compared with unstimulated macrophages. Scale bar, 2  $\mu$ M. **(B)** and **(C)** RNA-DNA FISH experiments performed in naive and endotoxin-tolerant RAW 264.7 macrophages with a subsequent exposure to LPS for the simultaneous detection of either the nascent miR-155 gene transcript and the miR-155 and miR-146a gene loci or the nascent miR-146a gene transcript and miR-155 and miR-146a gene loci. Arrows have been added to highlight miR-146a staining. Scale bar, 2  $\mu$ M. Graphs depict the percentage of endotoxin-tolerant and restimulated macrophages with miR-155 and miR-146a gene loci colocalization, monitoring in parallel the transcription status of the locus. The measurements were performed in three-dimensionally preserved cell nuclei, and 500 cells were scored in total in 3 independent experiments for each state.

calized were also affected. The transcriptional repressor C/EBP $\beta$  was increased 3-fold on both promoters at the stage of endotoxin tolerance (Fig. 3D), when compared with LPS-stimulated cells, also suggesting that this change may also affect the alleles that are not colocalized. Thus, changes on transcription factor binding observed at the stage of endotoxin tolerance may not be restricted



to the colocalized allele but also affect the noncolocalized allele, allowing reduced levels of expression.

*Colocalization of miR-155 and miR-146a gene loci is not induced in Akt1<sup>-/-</sup> macrophages*

To extend the aforementioned observations to primary cells, we used thioglycollate-elicited and LPS-stimulated peritoneal macrophages (TEPMs) from C57BL/6 mice. Restimulation of tolerized wild type (WT) TEPMs resulted in reduced expression of both the mature (Fig. 5A, left panel) and the microRNA transcripts (Fig. 5B, right panel) of miR-155 and miR-146a (Fig. 5A, 5B). Similar to RAW264.7 cells, in TEPMs, colocalization of the two miRNA loci at the stage of endotoxin tolerance was associated with transcriptional silencing because the colocalized alleles did not express their miRNA transcripts (Fig. 5C).

When Akt1<sup>-/-</sup> TEPMs were used as a genetic tool for abrogation of endotoxin tolerance (1) (Supplemental Fig. 4B), pri-miR-155 was more potently upregulated in response to secondary LPS stimulation, compared with WT macrophages (Fig. 5D). Furthermore, LPS-restimulated endotoxin-tolerant WT macrophages displayed enhanced induction of pri-miR-146a compared with Akt1<sup>-/-</sup> macrophages (Fig. 5E). The overall levels of pri- and mature miR-146a were lower in Akt1<sup>-/-</sup> macrophages, possibly due to the fact that they do not develop endotoxin tolerance (Supplemental Fig. 4C). To verify that the transcriptional machinery regulating transcription of these miRNAs is the same in primary macrophages as in RAW264.7 cells, we performed ChIP experiments to detect the recruitment of NFκBp65 and C/EBPβ on miR-155 and miR-146a regulatory elements. NFκBp65 was bound on both promoters upon LPS activation of primary naive macrophages, which

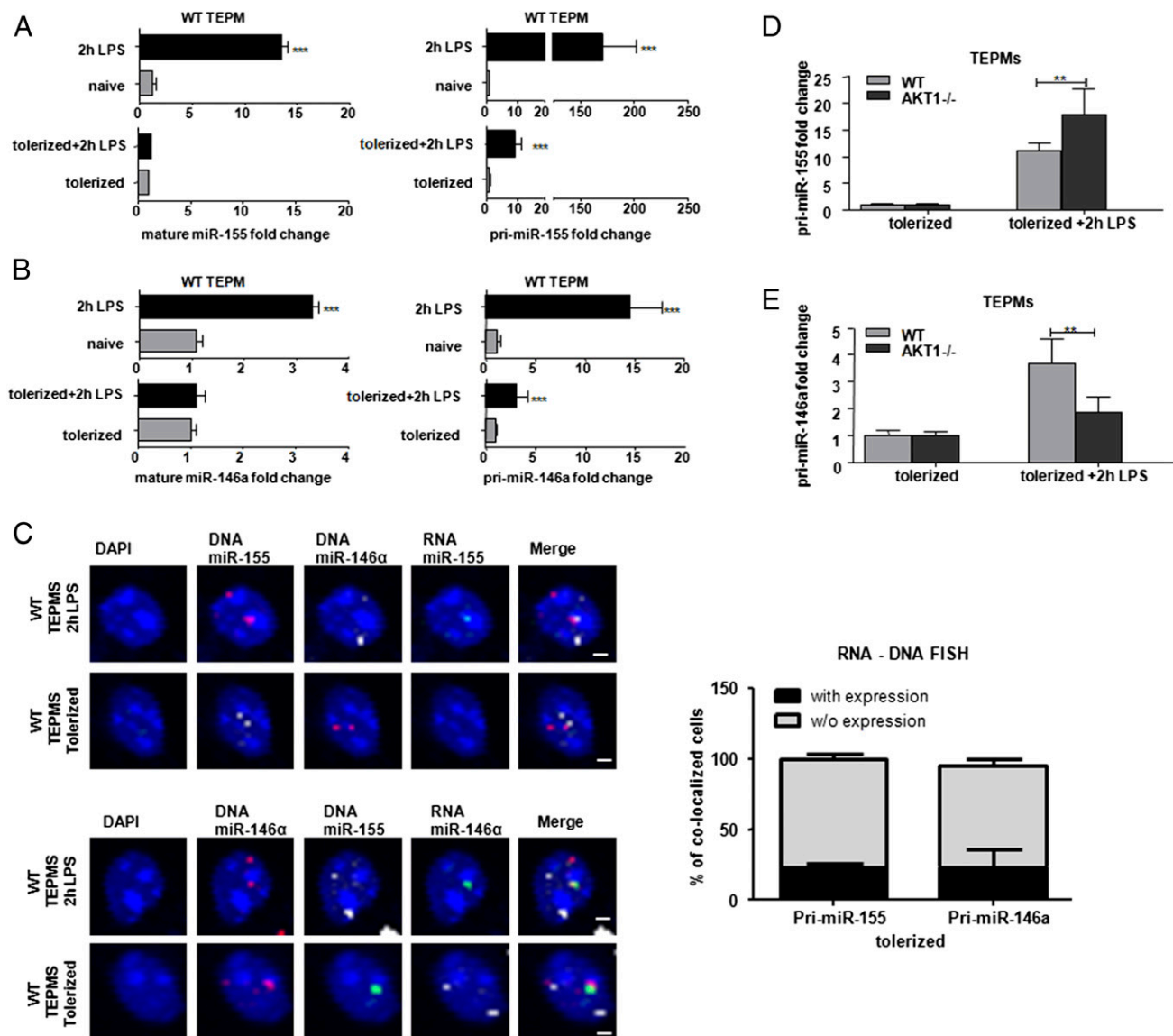


**FIGURE 5.** Differential expression profile of miR-155 and miR-146a in TEPMs of Akt1<sup>-/-</sup> mice. Expression of mature and microRNA transcripts of miR-155 (**A**) and miR-146a (**B**) was measured in naive, in 2-h-LPS-activated, in endotoxin-tolerant, and in endotoxin-tolerant primary TEPMs from WT mice restimulated for 2 h with LPS. (**C**) RNA-DNA FISH experiments performed in 2-h-LPS-activated and endotoxin-tolerant TEPMs for the simultaneous detection of either the nascent miR-155 gene transcript and the miR-155 and miR-146a gene loci or the nascent miR-146a gene transcript and miR-155 and miR-146a gene loci. Graph depicts the percentage of LPS-activated and endotoxin-tolerant macrophages with miR-155 and miR-146a gene loci, monitoring in parallel the transcription status of the locus. The measurements were performed in three-dimensionally preserved cell nuclei, and 500 cells were scored in total in 3 independent experiments for each state. Scale bar, 2 μM. (**D** and **E**) Expression of pri-miR-155 and pri-miR-146a was measured in WT and Akt1<sup>-/-</sup> macrophages at the stage of endotoxin tolerance and after secondary LPS stimulation. Results represent three independent experiments (± SD). \*\**p* = 0.01, \*\*\**p* = 0.001.

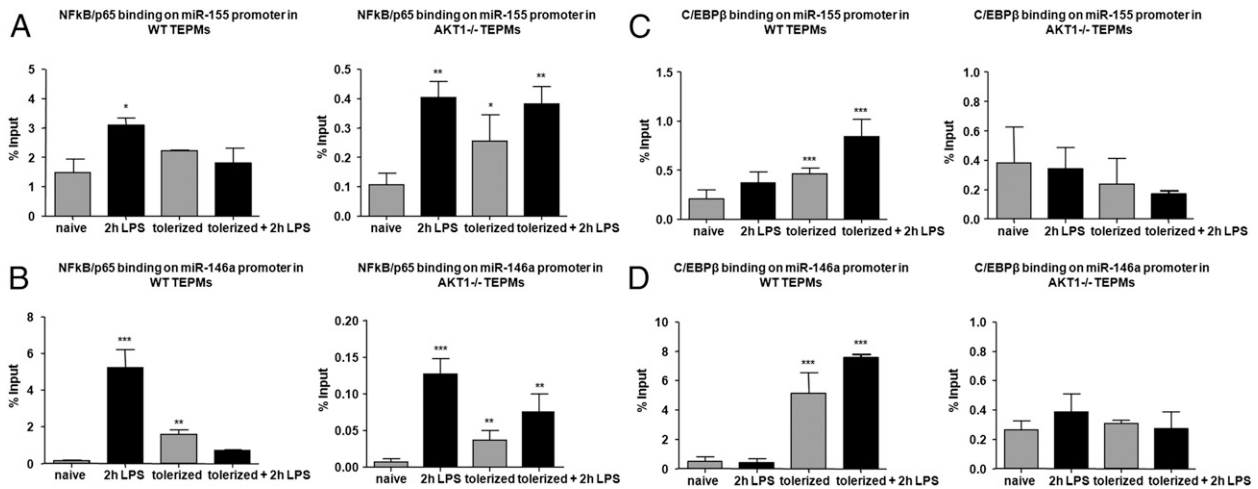


**FIGURE 6.** Differential regulation of NF- $\kappa$ B and C/EBP $\beta$  in TEPMs from Akt1<sup>-/-</sup> mice. Cell lysates from primary TEPMs at the naive state, following 2-h activation with LPS, at the endotoxin-tolerant state, and following 2-h activation with LPS of endotoxin-tolerant cells from WT or Akt1<sup>-/-</sup> mice were used in ChIP experiments using mAbs directed to NF- $\kappa$ Bp65 (**A** and **B**) and C/EBP $\beta$  (**C** and **D**). Precipitated DNA was amplified using primer pairs against regions of the miR-155 and miR-146a promoters. Results represent three independent experiments ( $\pm$  SD). \* $p$  = 0.05, \*\* $p$  = 0.01, \*\*\* $p$  = 0.001 compared with unstimulated macrophages.

was abrogated in LPS-restimulated, endotoxin-tolerant cells. In Akt1<sup>-/-</sup> macrophages, NF- $\kappa$ Bp65 was still recruited to the promoters of miR-155 and miR-146a genes (Fig. 6A, 6B, left panel), in accordance with their active transcription state. C/EBP $\beta$  was bound on both promoters of endotoxin-tolerant and restimulated tolerant WT macrophages, but not in Akt1<sup>-/-</sup> cells (Fig. 6C, 6D, right panel), further confirming its contribution in suppressing the expression of these miRs. According to the different expression profile of pri-miR-155 and pri-miR-146a, and altered NF- $\kappa$ B/p65 and C/EBP $\beta$  binding on their promoters in Akt1<sup>-/-</sup> macrophages,

no increase in the colocalization of miR-155 and miR-146a gene loci was observed. This finding further supports the significance of this association at the endotoxin-tolerant stage (Fig. 7A, 7B). All changes observed in these two gene loci are described in Fig. 8.

## Discussion

Endotoxin tolerance occurs to protect the organism from hyperactivation of innate immune responses, rendering macrophages hyporesponsive to subsequent stimuli. During sepsis or other major inflammatory stresses, a carefully orchestrated balance between

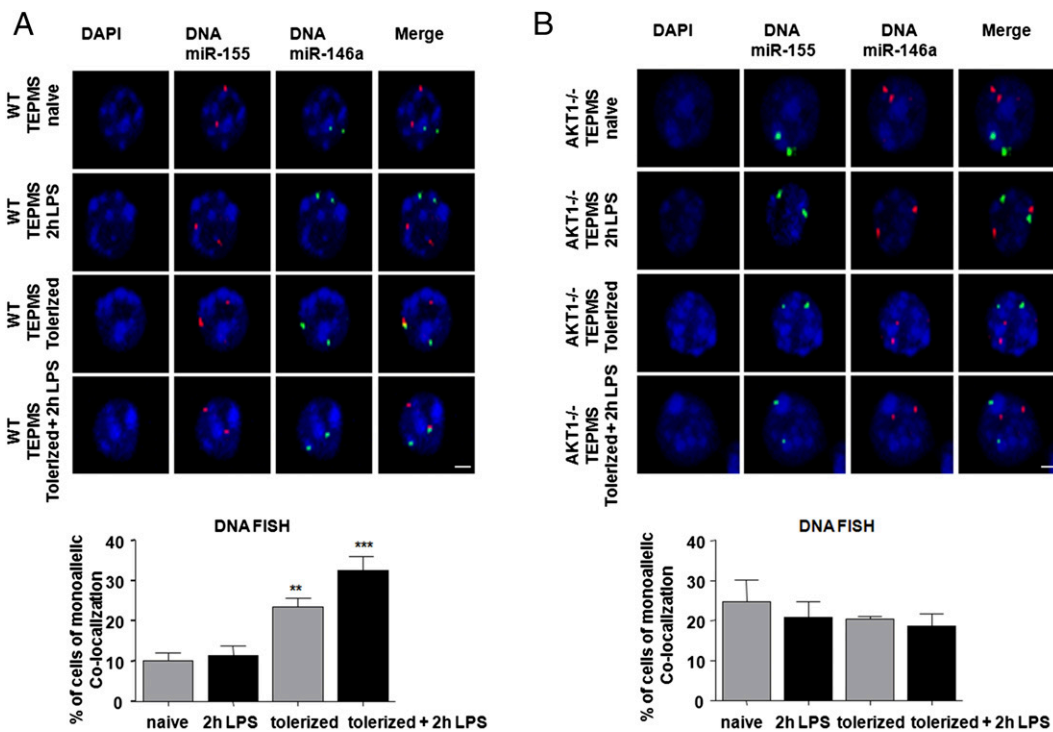


**FIGURE 7.** Colocalization of miR-155 and miR-146a is not induced in Akt1<sup>-/-</sup> macrophages. (**A** and **B**) DNA FISH experiments were performed in cell lysates from primary TEPMs at the naive state, following 2-h activation with LPS, at the endotoxin-tolerant state, and following 2-h activation with LPS of endotoxin-tolerant cells from WT (**A**) or Akt1<sup>-/-</sup> (**B**) mice for the detection of miR-155 and miR-146a gene loci. Graphs depict the percentage of TEPMs harboring colocalized miR-155 and miR-146a alleles. The measurements were performed in three-dimensionally preserved cell nuclei, and 500 cells were scored in total in 2 independent experiments for each state ( $\pm$  SD). Scale bar, 2  $\mu$ M. \*\* $p$  = 0.01, \*\*\* $p$  = 0.001 compared with unstimulated macrophages.

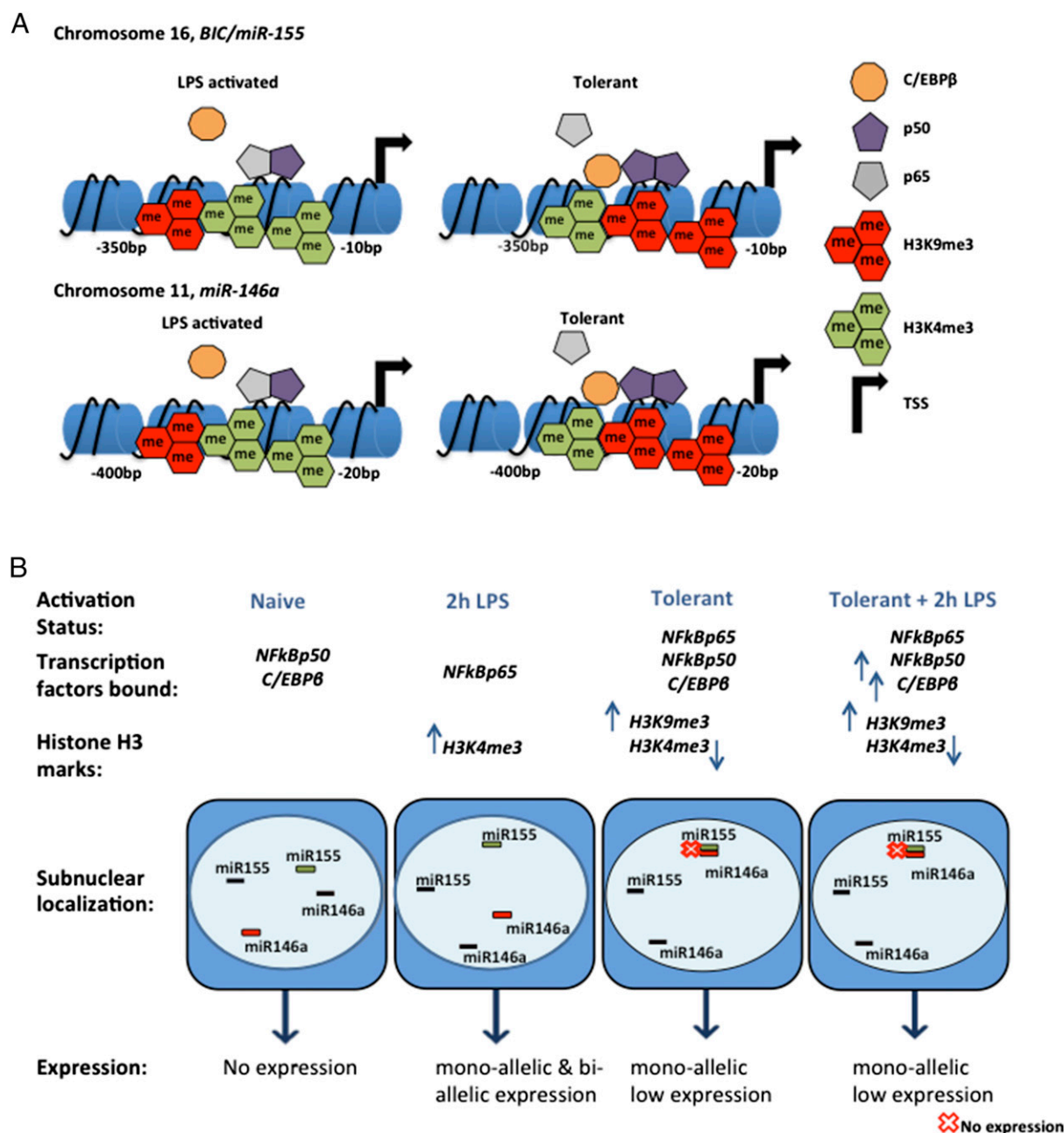


**FIGURE 8.** miR-155 and miR-146a share common regulatory events during macrophage activation and development of endotoxin tolerance. **(A)** Schematic representation of transcription factor binding and histone modification at the activation and endotoxin tolerance stages. **(B)** At the naive state, C/EBP $\beta$  and p50 were bound on the promoter of both miRNA genes. Upon LPS treatment, the transcription is induced from one or both alleles, which are marked with H3K4 trimethylation, and NF- $\kappa$ B-p65 was recruited while C/EBP $\beta$  binding was reduced. At the stage of endotoxin tolerance, one of the two alleles of each gene came into proximity conferring transcriptional silencing. C/EBP $\beta$  and NF $\kappa$ B-p50 occupied both miR-155 and miR-146a promoters in tolerant and restimulated tolerant macrophages, which were primarily marked by H3K9 trimethylation.

proinflammatory and anti-inflammatory mediators within the host organism is necessary to counteract and restore homeostasis. Deregulation of the balance between inflammatory response and tolerance can be lethal either through uncontrolled excessive inflammation leading to sepsis and extensive tissue damage or failure to defend against infectious organisms.

Development of endotoxin tolerance is characterized by significant changes in gene expression, chromatin structure, and histone modifications (58). Such global changes must be coordinated to ensure timely gene expression and limit energy and resource expenditure in the cell. At the signaling level, endotoxin tolerance involves suppression of TLR4 signals via negative regulatory proteins, anti-inflammatory cytokines/mediators, and

miRNAs. miR-155 and miR-146 play an essential role in this process. Although miR-155 contributes to the initial activation by targeting negative regulators of TLR signals (1), in the endotoxin tolerance phase it is involved in the negative regulation of macrophage activation partly by targeting TAB2, a mediator of IFN signaling (59). In contrast, miR-146a primarily contributes to suppression of activation signals and the development of endotoxin tolerance (13, 48, 49), and cooperates with miR-155 (9). In this article we demonstrate that at the stage of endotoxin tolerance these two miRNAs are regulated in a coordinated fashion that involves not only the same transcription factors and histone methylation marks, but also an intricate mechanism of monoallelic silencing.



Development of endotoxin tolerance in macrophages requires global changes in gene expression, which is reflected in global changes of H3 methylation. According to these changes, genes that are expressed acquire activatory H3 methyl marks, such as K4me3, and ones that require to be silenced acquire repressive methyl marks on H3, such as K9me3. In this study, we demonstrate that upon initial LPS stimulation, both miR genes were activated and acquired H3K4me3 marks (30). At the endotoxin-tolerant state, reduced H3K4me3 and increased H3K9me3 levels were observed at their promoters, indicating a silencing event (60). This is in agreement with genome-wide analysis showing loss of H3K4me3 marks from selected genes upon development of endotoxin tolerance (33, 34). Transcription of both miR-155 and miR-146a is regulated by the NF- $\kappa$ B transcription complex (10, 14). In this study, we demonstrated that whereas the p65 subunit of NF- $\kappa$ B was bound on their regulatory elements at the initial activation stage, LPS restimulation of endotoxin-tolerant macrophages resulted in recruitment of NF $\kappa$ Bp50, which is known to suppress transcription (61). In accordance with our findings, p50/NF- $\kappa$ B has previously been implicated in controlling macrophage inactivation and tolerance (62).

C/EBP $\beta$  was also found to bind on both promoters at the stage of endotoxin tolerance, and its presence was vital to suppress transcription of these genes. It is involved in both transcriptional activation and suppression, and recent evidence has implicated C/EBP $\beta$  in the transcriptional silencing of miRNAs such as let-7i, miR-145, and miR-155 (53, 63). Accessibility of promoters to C/EBP $\beta$  depends on H3 methylation status at the C/EBP $\beta$  binding region, as demonstrated previously (64, 65). Indeed, H3 methylation was detected in the proximal region of the miR-155 and miR-146a promoters (Fig. 8A). C/EBP $\beta$  has been shown to interact with the SWI/SNF nucleosome-remodeling complex, protein arginine *N*-methyltransferase-4 (66), which may potentially affect histone methylation patterns. Moreover, global changes in macrophage enhancer regions on H3K4 methylation marks partly depends on C/EBPs, as demonstrated by global nuclear run-on coupled to deep sequencing analysis (67, 68). These studies indicate a close association of H3 methylation changes and C/EBP $\beta$  binding, which may also apply on miR-155 and miR-146a promoters. Akt signaling regulates miRNA expression in macrophages (1, 47, 48, 53), although it has been demonstrated to regulate C/EBP $\beta$  activation either via direct phosphorylation (53), or indirectly via GSK3 (69) or p300/CBP (70). Interestingly, even though restimulation of endotoxin-tolerant macrophages with LPS induced binding of p65 and not of CEBP $\beta$  in Akt1<sup>-/-</sup> macrophages, induction of pri-miR-146a was lower in the absence of Akt1. This finding suggests that at that stage an alternative transcriptional repressive mechanism exists, which depends on Akt1 and affects miR-146a, but not miR-155.

Transcriptional regulation of genes can occur in a coordinated manner to ensure simultaneous regulation. For this purpose, gene loci come in proximity and are regulated by the same transcriptional machinery (71). miR-155 has been previously shown to participate in such transcription factories upon TNF- $\alpha$  stimulation (72). In this study, we demonstrated that miR-155 and miR-146a gene loci came into proximity at the stage of endotoxin tolerance. In addition, we showed that the associated alleles of miR-155 and miR-146a were not transcribed, suggesting a common silencing mechanism. In endotoxin-tolerant cells, expression was restricted mainly to one allele and biallelic expression was significantly reduced. Further confirmation of the significance of the association between miR-155 and miR-146a comes from the observation that in Akt1<sup>-/-</sup> macrophages, which fail to develop endotoxin tolerance (1), the association of these gene loci is not induced.

Overall, these results demonstrate a coordinated mechanism regulating the expression of miR-155 and miR-146a genes. Upon LPS treatment, the transcription is induced from one or both alleles, which are marked with H3K4 methylation and NF- $\kappa$ B-p65 recruitment. However, at the stage of endotoxin tolerance, one of the two alleles of each gene comes into proximity in a silencing environment (Fig. 8). Hence, our findings support the importance of coordinated regulation at the three-dimensional chromatin space of gene loci harboring miRNAs, during endotoxin tolerance. This mechanism may not be restricted to miR-155 and miR-146a but may apply to additional groups of genes that contribute to the same biological condition. Elucidating the molecular mechanisms that orchestrate endotoxin tolerance might lead to modulation of macrophage responses and the development of therapeutic interventions.

## Disclosures

The authors have no financial conflicts of interest.

## References

- Androulidaki, A., D. Iliopoulos, A. Arranz, C. Doxaki, S. Schworer, V. Zacharioudaki, A. N. Margioris, P. N. Tsihliis, and C. Tsatsanis. 2009. The kinase Akt1 controls macrophage response to lipopolysaccharide by regulating microRNAs. *Immunity* 31: 220–231.
- El Gazzar, M., and C. E. McCall. 2010. MicroRNAs distinguish translational from transcriptional silencing during endotoxin tolerance. *J. Biol. Chem.* 285: 20940–20951.
- Liu, Y., Q. Chen, Y. Song, L. Lai, J. Wang, H. Yu, X. Cao, and Q. Wang. 2011. MicroRNA-98 negatively regulates IL-10 production and endotoxin tolerance in macrophages after LPS stimulation. *FEBS Lett.* 585: 1963–1968.
- Quinn, E. M., J. Wang, and H. P. Redmond. 2012. The emerging role of microRNA in regulation of endotoxin tolerance. *J. Leukoc. Biol.* 91: 721–727.
- Chassin, C., M. Kocur, J. Pott, C. U. Duerr, D. Gütle, M. Lotz, and M. W. Horne. 2010. miR-146a mediates protective innate immune tolerance in the neonate intestine. *Cell Host Microbe* 8: 358–368.
- Banerjee, S., J. Meng, S. Das, A. Krishnan, J. Haworth, R. Charboneau, Y. Zeng, S. Ramakrishnan, and S. Roy. 2013. Morphine induced exacerbation of sepsis is mediated by tempering endotoxin tolerance through modulation of miR-146a. *Sci. Rep.* 3: 1977.
- Alexander, M., R. Hu, M. C. Runtsch, D. A. Kagele, T. L. Mosbrugger, T. Tolmachova, M. C. Seabra, J. L. Round, D. M. Ward, and R. M. O'Connell. 2015. Exosome-delivered microRNAs modulate the inflammatory response to endotoxin. *Nat. Commun.* 6: 7321.
- Jurado-Camino, T., R. Córdoba, L. Esteban-Burgos, E. Hernández-Jiménez, V. Toledoano, J. A. Hernandez-Rivas, E. Ruiz-Sainz, T. Cobo, M. Siliceo, R. Perez de Diego, et al. 2015. Chronic lymphocytic leukemia: a paradigm of innate immune cross-tolerance. *J. Immunol.* 194: 719–727.
- Schulte, L. N., A. J. Westermann, and J. Vogel. 2013. Differential activation and functional specialization of miR-146 and miR-155 in innate immune sensing. *Nucleic Acids Res.* 41: 542–553.
- Taganov, K. D., M. P. Boldin, K. J. Chang, and D. Baltimore. 2006. NF-kappaB-dependent induction of microRNA miR-146, an inhibitor targeted to signaling proteins of innate immune responses. *Proc. Natl. Acad. Sci. USA* 103: 12481–12486.
- Kagiyama, T., and S. Nakamura. 2013. Expression profiling of microRNAs in RAW264.7 cells treated with a combination of tumor necrosis factor alpha and RANKL during osteoclast differentiation. *J. Periodontol. Res.* 48: 373–385.
- Kutty, R. K., C. N. Nagineni, W. Samuel, C. Vijayasarathy, C. Jaworski, T. Duncan, J. E. Cameron, E. K. Flemington, J. J. Hooks, and T. M. Redmond. 2013. Differential regulation of microRNA-146a and microRNA-146b-5p in human retinal pigment epithelial cells by interleukin-1 $\beta$ , tumor necrosis factor- $\alpha$ , and interferon- $\gamma$ . *Mol. Vis.* 19: 737–750.
- Nahid, M. A., K. M. Pauley, M. Satoh, and E. K. Chan. 2009. miR-146a is critical for endotoxin-induced tolerance: IMPLICATION IN INNATE IMMUNITY. *J. Biol. Chem.* 284: 34590–34599.
- O'Connell, R. M., K. D. Taganov, M. P. Boldin, G. Cheng, and D. Baltimore. 2007. MicroRNA-155 is induced during the macrophage inflammatory response. *Proc. Natl. Acad. Sci. USA* 104: 1604–1609.
- Perry, M. M., A. E. Williams, E. Tsiotou, H. M. Larner-Svensson, and M. A. Lindsay. 2009. Divergent intracellular pathways regulate interleukin-1 $\beta$ -induced miR-146a and miR-146b expression and chemokine release in human alveolar epithelial cells. *FEBS Lett.* 583: 3349–3355.
- Kutty, R. K., C. N. Nagineni, W. Samuel, C. Vijayasarathy, J. J. Hooks, and T. M. Redmond. 2010. Inflammatory cytokines regulate microRNA-155 expression in human retinal pigment epithelial cells by activating JAK/STAT pathway. *Biochem. Biophys. Res. Commun.* 402: 390–395.
- Pauley, K. M., M. Satoh, A. L. Chan, M. R. Bub, W. H. Reeves, and E. K. Chan. 2008. Upregulated miR-146a expression in peripheral blood mononuclear cells from rheumatoid arthritis patients. *Arthritis Res. Ther.* 10: R101.
- Stanczyk, J., D. M. Pedrioli, F. Brentano, O. Sanchez-Pernaute, C. Kolling, R. E. Gay, M. Detmar, S. Gay, and D. Kyburz. 2008. Altered expression of



- MicroRNA in synovial fibroblasts and synovial tissue in rheumatoid arthritis. *Arthritis Rheum.* 58: 1001–1009.
19. Wang, G., L. S. Tam, B. C. Kwan, E. K. Li, K. M. Chow, C. C. Luk, P. K. Li, and C. C. Szeto. 2012. Expression of miR-146a and miR-155 in the urinary sediment of systemic lupus erythematosus. *Clin. Rheumatol.* 31: 435–440.
  20. Wang, G., B. C. Kwan, F. M. Lai, K. M. Chow, P. K. Li, and C. C. Szeto. 2011. Elevated levels of miR-146a and miR-155 in kidney biopsy and urine from patients with IgA nephropathy. *Dis. Markers* 30: 171–179.
  21. Kin, K., S. Miyagawa, S. Fukushima, Y. Shirakawa, K. Torikai, K. Shimamura, T. Daimon, Y. Kawahara, T. Kuratani, and Y. Sawa. 2012. Tissue- and plasma-specific MicroRNA signatures for atherosclerotic abdominal aortic aneurysm. *J. Am. Heart Assoc.* 1: e000745.
  22. Tsatsanis, C., J. Bobjer, H. Rastkhani, E. Dermitzaki, M. Katrinaki, A. N. Margioris, Y. L. Giwerzman, and A. Giwerzman. 2015. Serum miR-155 as a potential biomarker of male fertility. *Hum. Reprod.* 30: 853–860.
  23. Xie, Y. F., R. Shu, S. Y. Jiang, D. L. Liu, and X. L. Zhang. 2011. Comparison of microRNA profiles of human periodontal diseased and healthy gingival tissues. *Int. J. Oral Sci.* 3: 125–134.
  24. Corral-Fernández, N. E., M. Salgado-Bustamante, M. E. Martínez-Leija, N. Cortez-Espinosa, M. H. García-Hernández, E. Reynaga-Hernández, R. Quezada-Calvillo, and D. P. Portales-Pérez. 2013. Dysregulated miR-155 expression in peripheral blood mononuclear cells from patients with type 2 diabetes. *Exp. Clin. Endocrinol. Diabetes* 121: 347–353.
  25. Doxakis, E. 2013. Principles of miRNA-target regulation in metazoan models. *Int. J. Mol. Sci.* 14: 16280–16302.
  26. Etzrodt, M., V. Cortez-Retamozo, A. Newton, J. Zhao, A. Ng, M. Wildgruber, P. Romero, T. Wurdinger, R. Xavier, F. Geissmann, et al. 2012. Regulation of monocyte functional heterogeneity by miR-146a and Relb. *Cell Reports* 1: 317–324.
  27. Kluiver, J., A. van den Berg, D. de Jong, T. Blokzijl, G. Harms, E. Bouwman, S. Jacobs, S. Poppema, and B. J. Kroesen. 2007. Regulation of pri-microRNA BIC transcription and processing in Burkitt lymphoma. *Oncogene* 26: 3769–3776.
  28. Strahl, B. D., and C. D. Allis. 2000. The language of covalent histone modifications. *Nature* 403: 41–45.
  29. Jenuwein, T., and C. D. Allis. 2001. Translating the histone code. *Science* 293: 1074–1080.
  30. Santos-Rosa, H., R. Schneider, A. J. Bannister, J. Sherriff, B. E. Bernstein, N. C. Emre, S. L. Schreiber, J. Mellor, and T. Kouzarides. 2002. Active genes are tri-methylated at K4 of histone H3. *Nature* 419: 407–411.
  31. Bernstein, B. E., M. Kamal, K. Lindblad-Toh, S. Bekiranov, D. K. Bailey, D. J. Huebert, S. McMahon, E. K. Karlsson, E. J. Kulbokas, III, T. R. Gingeras, et al. 2005. Genomic maps and comparative analysis of histone modifications in human and mouse. *Cell* 120: 169–181.
  32. Schneider, R., A. J. Bannister, F. A. Myers, A. W. Thorne, C. Crane-Robinson, and T. Kouzarides. 2004. Histone H3 lysine 4 methylation patterns in higher eukaryotic genes. *Nat. Cell Biol.* 6: 73–77.
  33. Foster, S. L., D. C. Hargreaves, and R. Medzhitov. 2007. Gene-specific control of inflammation by TLR-induced chromatin modifications. *Nature* 447: 972–978.
  34. Foster, S. L., and R. Medzhitov. 2009. Gene-specific control of the TLR-induced inflammatory response. *Clin. Immunol.* 130: 7–15.
  35. Lyn-Kew, K., E. Rich, X. Zeng, H. Wen, S. L. Kunkel, M. W. Newstead, U. Bhan, and T. J. Standiford. 2010. IRAK-M regulates chromatin remodeling in lung macrophages during experimental sepsis. *PLoS One* 5: e11145.
  36. Jing, J., I. V. Yang, L. Hui, J. A. Patel, C. M. Evans, R. Prikeris, L. Kobzik, B. P. O'Connor, and D. A. Schwartz. 2013. Role of macrophage receptor with collagenous structure in innate immune tolerance. *J. Immunol.* 190: 6360–6367.
  37. Belmont, A. S. 2014. Large-scale chromatin organization: the good, the surprising, and the still perplexing. *Curr. Opin. Cell Biol.* 26: 69–78.
  38. Hübner, M. R., M. A. Eckersley-Maslin, and D. L. Spector. 2013. Chromatin organization and transcriptional regulation. *Curr. Opin. Genet. Dev.* 23: 89–95.
  39. Merkenschlager, M., and D. T. Odum. 2013. CTCF and cohesin: linking gene regulatory elements with their targets. *Cell* 152: 1285–1297.
  40. Hübner, M. R., and D. L. Spector. 2010. Chromatin dynamics. *Annu. Rev. Biophys.* 39: 471–489.
  41. Dekker, J., M. A. Marti-Renom, and L. A. Mirny. 2013. Exploring the three-dimensional organization of genomes: interpreting chromatin interaction data. *Nat. Rev. Genet.* 14: 390–403.
  42. Deligianni, C., and C. G. Spilianakis. 2012. Long-range genomic interactions epigenetically regulate the expression of a cytokine receptor. *EMBO Rep.* 13: 819–826.
  43. Spilianakis, C. G., and R. A. Flavell. 2006. Molecular biology. Managing associations between different chromosomes. *Science* 312: 207–208.
  44. Spilianakis, C. G., M. D. Lalioti, T. Town, G. R. Lee, and R. A. Flavell. 2005. Interchromosomal associations between alternatively expressed loci. *Nature* 435: 637–645.
  45. Mao, C., E. G. Tili, M. Dose, M. C. Haks, S. E. Bear, I. Maroulakou, K. Horie, G. A. Gaitanaris, V. Fidanza, T. Ludwig, et al. 2007. Unequal contribution of Akt isoforms in the double-negative to double-positive thymocyte transition. *J. Immunol.* 178: 5443–5453.
  46. Maroulakou, I. G., W. Oemler, S. P. Naber, and P. N. Tschlis. 2007. Akt1 ablation inhibits, whereas Akt2 ablation accelerates, the development of mammary adenocarcinomas in mouse mammary tumor virus (MMTV)-ErbB2/neu and MMTV-polyoma middle T transgenic mice. *Cancer Res.* 67: 167–177.
  47. Arranz, A., A. Androulidaki, V. Zacharioudaki, C. Martinez, A. N. Margioris, R. P. Gomariz, and C. Tsatsanis. 2008. Vasoactive intestinal peptide suppresses toll-like receptor 4 expression in macrophages via Akt1 reducing their responsiveness to lipopolysaccharide. *Mol. Immunol.* 45: 2970–2980.
  48. Vergadi, E., K. Vaporiidi, E. E. Theodorakis, C. Doxaki, E. Lagoudaki, E. Ieronymaki, V. I. Alexaki, M. Helms, E. Kondili, B. Soennichsen, et al. 2014. Akt2 deficiency protects from acute lung injury via alternative macrophage activation and miR-146a induction in mice. *J. Immunol.* 192: 394–406.
  49. Nahid, M. A., M. Satoh, and E. K. Chan. 2011. Mechanistic role of microRNA-146a in endotoxin-induced differential cross-regulation of TLR signaling. *J. Immunol.* 186: 1723–1734.
  50. Chen, D., L. Y. Fu, Z. Zhang, G. Li, H. Zhang, L. Jiang, A. P. Harrison, H. P. Shanahan, C. Klukas, H. Y. Zhang, et al. 2014. Dissecting the chromatin interactome of microRNA genes. *Nucleic Acids Res.* 42: 3028–3043.
  51. Yin, Q., X. Wang, J. McBride, C. Fewell, and E. Flemington. 2008. B-cell receptor activation induces BIC/miR-155 expression through a conserved AP-1 element. *J. Biol. Chem.* 283: 2654–2662.
  52. Chen, Y., F. Siegel, S. Kipschull, B. Haas, H. Fröhlich, G. Meister, and A. Pfeifer. 2013. miR-155 regulates differentiation of brown and beige adipocytes via a bistable circuit. *Nat. Commun.* 4: 1769.
  53. Sachdeva, M., Q. Liu, J. Cao, Z. Lu, and Y. Y. Mo. 2012. Negative regulation of miR-145 by C/EBP- $\beta$  through the Akt pathway in cancer cells. *Nucleic Acids Res.* 40: 6683–6692.
  54. Augui, S., E. P. Nora, and E. Heard. 2011. Regulation of X-chromosome inactivation by the X-inactivation centre. *Nat. Rev. Genet.* 12: 429–442.
  55. Chess, A. 2012. Mechanisms and consequences of widespread random monoallelic expression. *Nat. Rev. Genet.* 13: 421–428.
  56. Rodríguez, I. 2013. Singular expression of olfactory receptor genes. *Cell* 155: 274–277.
  57. Yang, P. K., and M. I. Kuroda. 2007. Noncoding RNAs and intranuclear positioning in monoallelic gene expression. *Cell* 128: 777–786.
  58. Medzhitov, R., and T. Horng. 2009. Transcriptional control of the inflammatory response. *Nat. Rev. Immunol.* 9: 692–703.
  59. Ceppi, M., P. M. Pereira, I. Dunand-Sauthier, E. Barras, W. Reith, M. A. Santos, and P. Pierre. 2009. MicroRNA-155 modulates the interleukin-1 signaling pathway in activated human monocyte-derived dendritic cells. *Proc. Natl. Acad. Sci. USA* 106: 2735–2740.
  60. Lachner, M., D. O'Carroll, S. Rea, K. Mechtler, and T. Jenuwein. 2001. Methylation of histone H3 lysine 9 creates a binding site for HP1 proteins. *Nature* 410: 116–120.
  61. Biswas, S. K., and E. Lopez-Collazo. 2009. Endotoxin tolerance: new mechanisms, molecules and clinical significance. *Trends Immunol.* 30: 475–487.
  62. Porta, C., M. Rimoldi, G. Raes, L. Brys, P. Ghezzi, D. Di Liberto, F. Dieli, S. Ghisletti, G. Natoli, P. De Baetselier, et al. 2009. Tolerance and M2 (alternative) macrophage polarization are related processes orchestrated by p50 nuclear factor kappaB. *Proc. Natl. Acad. Sci. USA* 106: 14978–14983.
  63. O'Hara, S. P., P. L. Splinter, G. B. Gajdos, C. E. Trussoni, M. E. Fernandez-Zapico, X. M. Chen, and N. F. LaRusso. 2010. NFkappaB p50-CCAAT/enhancer-binding protein beta (C/EBPbeta)-mediated transcriptional repression of microRNA let-7i following microbial infection. *J. Biol. Chem.* 285: 216–225.
  64. Wang, F., M. Demura, Y. Cheng, A. Zhu, S. Karashima, T. Yoneda, Y. Demura, Y. Maeda, M. Namiki, K. Ono, et al. 2014. Dynamic CCAAT/enhancer binding protein-associated changes of DNA methylation in the angiotensinogen gene. *Hypertension* 63: 281–288.
  65. Pham, T. H., C. Benner, M. Lichtinger, L. Schwarzfischer, Y. Hu, R. Andreesen, W. Chen, and M. Rehli. 2012. Dynamic epigenetic enhancer signatures reveal key transcription factors associated with monocytic differentiation states. *Blood* 119: e161–e171.
  66. Kowenz-Leutz, E., O. Pless, G. Dittmar, M. Knoblich, and A. Leutz. 2010. Crosstalk between C/EBPbeta phosphorylation, arginine methylation, and SWI/SNF/Mediator implies an indexing transcription factor code. *EMBO J.* 29: 1105–1115.
  67. Kaikkonen, M. U., N. J. Spann, S. Heinz, C. E. Romanoski, K. A. Allison, J. D. Stender, H. B. Chun, D. F. Tough, R. K. Prinjha, C. Benner, and C. K. Glass. 2013. Remodeling of the enhancer landscape during macrophage activation is coupled to enhancer transcription. *Mol. Cell* 51: 310–325.
  68. Romanoski, C. E., V. M. Link, S. Heinz, and C. K. Glass. 2015. Exploiting genomics and natural genetic variation to decode macrophage enhancers. *Trends Immunol.* 36: 507–518.
  69. Piwien-Pilipuk, G., D. Van Mater, S. E. Ross, O. A. MacDougald, and J. Schwartz. 2001. Growth hormone regulates phosphorylation and function of CCAAT/enhancer-binding protein beta by modulating Akt and glycogen synthase kinase-3. *J. Biol. Chem.* 276: 19664–19671.
  70. Guo, S., S. B. Cichy, X. He, Q. Yang, M. Ragland, A. K. Ghosh, P. F. Johnson, and T. G. Untermyer. 2001. Insulin suppresses transactivation by CAAT/enhancer-binding proteins beta (C/EBPbeta). Signaling to p300/CREB-binding protein by protein kinase B disrupts interaction with the major activation domain of C/EBPbeta. *J. Biol. Chem.* 276: 8516–8523.
  71. Williams, A., C. G. Spilianakis, and R. A. Flavell. 2010. Interchromosomal association and gene regulation in trans. *Trends Genet.* 26: 188–197.
  72. Papanonitis, A., T. Kohro, S. Baboo, J. D. Larkin, B. Deng, P. Short, S. Tsutsumi, S. Taylor, Y. Kanki, M. Kobayashi, et al. 2012. TNF $\alpha$  signals through specialized factories where responsive coding and miRNA genes are transcribed. *EMBO J.* 31: 4404–4414.